A Novel Tunable Window for Signal Processing Applications

Debanjan Bhattacharjee and Sujit Kumar Sahoo, *Senior Member, IEEE*

***Abstract*—This work introduces a novel four-parameter window function constructed as a structured product of exponential hyperbolic tan, hyperbolic cosine, and polynomial tapering functions. The proposed window adopts a targeted spectral strategy, prioritizing the suppression of near-in side-lobes that dominate practical performance while allowing controlled relaxation in the far-out spectrum when required. The window's ability to achieve exponential spectral decay or equi-ripple behavior through tuning has also been demonstrated. A comparative analysis against the Hamming window, Taylor window, Blackman-Harris window, Dolph-Chebyshev window, fractional Kaiser, and the Kaiser window demonstrated the window's ability to match the first side-lobe suppression of the Kaiser window and the Taylor window at a 4% and 26% narrower main-lobe width, respectively. It is also demonstrated that for small window lengths, the main-lobe is narrower than or roughly the same as that for the Hamming window, while simultaneously achieving a side-lobe suppression same as that of the Kaiser and Dolph-Chebyshev windows. Further analysis showed that, with roughly the same main-lobe width as the fractional Kaiser window, the proposed window achieves $17\,\mathrm{dB}$ and $23\,\mathrm{dB}$ higher near-side-lobe suppression for window lengths of 51 and 31 taps, respectively.**

***Index Terms*—window function, exponential hyperbolic-tan, hyperbolic–cosine, targeted spectral strategy.**

I. Introduction

Window functions are an important aspect in the fields of communications, image, and signal processing. They are deterministic weighting sequences used to control spectral leakage, side-lobe behavior, and numerical stability when finite-length data are processed in transform-based or optimization-based systems. Their utility extends beyond classical FIR filter design [1], wherein the window functions are used to mitigate the oscillations caused by truncation as a manifestation of Gibbs' phenomenon [2], to any application where truncation, segmentation, or finite observation imposes artificial discontinuities. Window functions in image processing are used as spatial weighting masks to smoothly taper pixel values, eliminate spatial domain ringing, and reduce boundary artifacts. They are commonly applied in image fusion and blending [3], CT imaging using Radon transform and filtered backprojection [4], local frequency analysis (STFT/FFT) [5], feature extraction and template matching [6], and patch-based reconstruction or super-resolution to suppress seams, ringing, and spectral leakage while preserving detail. In signal processing, window shapes time–frequency representations, stabilize spectral estimation, and control bias–variance trade-offs in periodograms [7] and parametric estimators. In communication systems, they influence pulse shaping [8], reduce out-of-band emissions, suppress interference in multi-carrier modulation, and improve synchronization and channel estimation under finite observation constraints.

Window functions are utilized by multiplying them to an infinite length sequence or function $f(x)$, which in turn produces a finite length weighted segment of the same sequence or function of length M, denoted by $g(x)_M$.

$$g(x)_M = f(x)w[n] \tag{1}$$

Here, $w[n]$ is the window function spanning an interval of length M, mathematically given by:

$$w[n] = \begin{cases} y[n], & 0 \le n \le M-1 \\ 0, & \text{otherwise} \end{cases} \tag{2}$$

where $y[n]$ represents the window values within the given sample length.

A. Window Functions in Literature

Window functions can be categorized into two distinct categories depending on their tunability. These categories are fixed windows and adjustable windows. Fixed windows are characterized solely by the length of the window M, making them impractical for applications with varying spectral characteristics. Some widely used examples of fixed windows include Rectangular, Von Hann, Blackman, Hamming [1], Bartlett [7], Blackman-Harris [9], Bartlett-Hann [10], and Lanczos [11]. The rigidity of fixed windows is countered by designs that incorporate adjustable parameters, yielding adjustable windows. However, even these adjustable windows face inherent limitations. The Dolph-Chebyshev [12] window is designed to have the smallest possible width of the main-lobe for a given level of the side lobe attenuation. However, due to the enforcement of an equi-ripple behavior, the window sacrifices main-lobe width for high attenuation at the far-side lobes. The widely used Kaiser [13] window and its more modern derivatives like Kaiser–Hamming [14], Kaiser–Von Hann [15], modified Kaiser [16], and fractional Kaiser [17] windows eliminate these edge impulses, but at the cost of an appreciably larger transition bandwidth for the same attenuation levels of the Dolph-Chebyshev window. The fractional Kaiser window is used for comparative analysis in this study, as it alters the underlying kernel of the Kaiser window via a fractional-order Bessel function, yielding a smoother and more intrinsic control over side-lobe decay that does not rely on heuristic ripple equalization or piecewise optimization. As a result, for comparable window lengths and main-lobe widths, it consistently achieves higher ripple suppression

Debanjan Bhattacharjee is with the School of Electrical Sciences, Indian Institute of Technology, Goa, India (e-mail: debanjan25242104@iitgoa.ac.in).

Dr. Sujit Kr. Sahoo is with the with the School of Electrical Sciences, Indian Institute of Technology, Goa, India (e-mail: sujit@iitgoa.ac.in).

and higher minimum stop-band attenuation than both hybrid (Kaiser–Hamming, Kaiser–Von Hann) and parametric extensions of the Kaiser window, like the modified Kaiser, while strictly subsuming the classical Kaiser as a special case. Another window of particular interest is the Taylor window [18], which demonstrates a targeted suppression strategy unlike the above-mentioned windows. For a specified window length, the Taylor window provides the option to choose the specific near-lobe suppression level (sll) and the number of near-lobes that should achieve the specific attenuation level ($\bar{n}$), while allowing relaxation for the far-out lobes. This feature allows it to achieve acceptable levels of attenuation at narrow main-lobe widths. Adjustable windows have been the subject of extensive research till date, and efforts are being made to enhance the effectiveness of window functions across a range of applications [19]–[22].

There exists a trade-off between the main-lobe width and the side-lobe suppression level in window functions. Most window functions impose an equi-ripple behavior, owing to which, as the side-lobe suppression increases, so does the main-lobe width. The Taylor window departs from this equi-ripple behavior, as discussed above. However, for narrower window lengths, the main-lobe width corresponding to the Taylor window remains wider than the Hamming window, which is a benchmark for small main-lobe width. The proposed window design demonstrates a main-lobe width narrower than that of the Hamming window for a smaller window length (e.g., 31 taps), while achieving a much higher near-in side-lobe attenuation than it. Like the Taylor window, the proposed window demonstrates a targeted suppression strategy, in which, instead of uniformly lowering the entire stop-band, it concentrates its maximum attenuation on the critical near-lobe region. Targeted side-lobe suppression is of paramount importance in high-precision, low-latency applications. Similar side-lobe suppression requirements arise in applications such as biomedical ultrasound [23], where suppressing near-in clutter is vital for lateral resolution, and cognitive radio [24], where narrower guard bands maximize spectral efficiency. Furthermore, in Synthetic Aperture Radar (SAR) [25], and antenna array design [26], the suppression of near-in side-lobes while maintaining a narrow main-lobe width ensures high-dynamic-range target detection and precise beam-pattern control without time-domain artifacts.

The novelty of this work lies in the window's ability to demonstrate near-lobe-targeted suppression, equi-ripple behavior, or exponential spectral decay, depending on parameter tuning. An equi-ripple behavior ensures that the approximation error tends to be somewhat more uniformly distributed with respect to frequency. Exponential spectral decay reduces far-out spectral leakage more rapidly, leading to improved side-lobe suppression and dynamic range. This ability to alternate between all three regimes is uncharacteristic of existing window designs to our knowledge.

The remainder of the paper is structured as follows. The mathematical expression of the proposed window function is given in Section II. Section III discusses the effects of tuning the four parameters and compares the proposed window function with conventional and new window functions. Finally, Section IV concludes the discussion, followed by the bibliography.

II. Proposed Window Function

The proposed window function is a multiplicative combination of three functions, which are given as:

$$
\begin{aligned}
y_1[n] &= e^{-\tanh\left(\alpha(\frac{2n}{M-1})^2\right)} - e^{-1} \\
y_2[n] &= 1 - \cosh^{-\gamma}\left(\exp\left(-(\tfrac{2n-M+1}{\sigma(M-1)})^2\right)\right) \\
y_3[n] &= \left(1 - \left(\frac{\frac{2n}{M-1} - 1}{\max\limits_{0\le k<M-1}\left|\frac{2k}{M-1} - 1\right|}\right)^2\right)^{\beta} \\
w[n] &= y_1[n]\, y_2[n]\, y_3[n] \qquad n \in [0, M-1]
\end{aligned}
\tag{3}
$$

The discrete factors $y_1[n]$, $y_2[n]$, and $y_3[n]$ are real, bounded, and symmetric sequences obtained by sampling smooth, even continuous kernels over $n \in \{0, \ldots, M-1\}$. The term $y_1[n]$ is an exponential–hyperbolic component that controls central concentration and main-lobe width, $y_2[n]$ is a nested exponential–hyperbolic attenuation term governing side-lobe suppression and far-out spectral decay, and $y_3[n]$ is a compactly supported polynomial taper enforcing smooth roll-off and endpoint regularity. Their product $w[n]$ therefore defines a finite-energy, non-negative, symmetric discrete window whose spectral characteristics arise from a clear separation of roles between central shaping, decay control, and boundary smoothness.

III. Results & Discussions

In this section, we investigate the characteristics of the window function dependent on the parameters (α, β, γ, σ) and perform a comparative analysis of the proposed window against a few other windows.

A. Window Characteristics

Here, we investigate the effects of the tuning parameters on the time and frequency domain spectral characteristics of the proposed window function. The frequency domain characteristics are demonstrated by taking an 8192-point FFT for higher resolution. The metrics by which we demonstrate the frequency domain window characteristics are the first side-lobe attenuation A_s, half main-lobe width $\Delta\omega$, and the attenuation at π rad/s, denoted by A_π.

From the figures 1 through 4, we can infer that the parameter α controls the sharpness of the central taper through the hyperbolic–tangent term, where larger values produce steeper edge decay and wider transition bandwidths with stronger spectral fall-off. The targeted suppression of the near-in-side lobe is mainly controlled by α, as seen in the case of $\alpha = 0.1$. The parameter β governs edge smoothness via the polynomial factor, with higher values yielding lower side-lobes and faster spectral decay. Hence, the ability of the window function to achieve exponential spectral decay or an equi-ripple behavior is mostly governed by β. The parameter γ mainly regularizes the side-lobe envelope, improving attenuation with little effect on transition width. Finally, σ sets the spread of the Gaussian-like taper. A smaller σ broadens the main lobe and increases

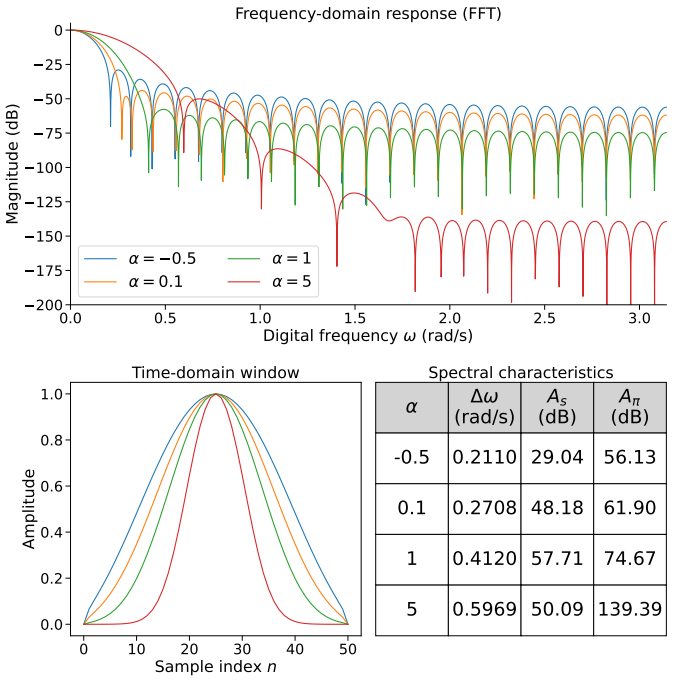

α	$\Delta\omega$ (rad/s)	A_s (dB)	A_π (dB)
-0.5	0.2110	29.04	56.13
0.1	0.2708	48.18	61.90
1	0.4120	57.71	74.67
5	0.5969	50.09	139.39

Fig. 1: Dependence of filter characteristics on α when β = 0.5, γ = 0.1 and σ = 0.913.

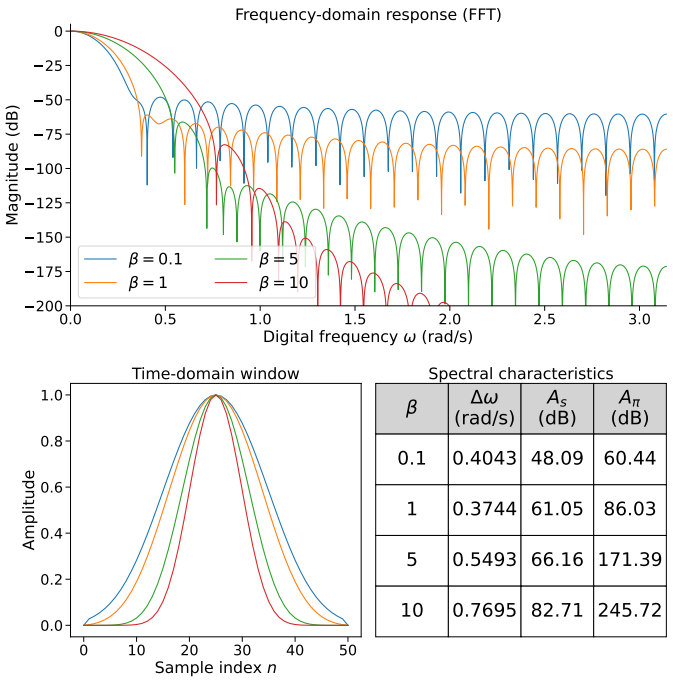

β	$\Delta\omega$ (rad/s)	A_s (dB)	A_π (dB)
0.1	0.4043	48.09	60.44
1	0.3744	61.05	86.03
5	0.5493	66.16	171.39
10	0.7695	82.71	245.72

Fig. 2: Dependence of filter characteristics on β when α = 0.8, γ = 0.5 and σ = 0.913.

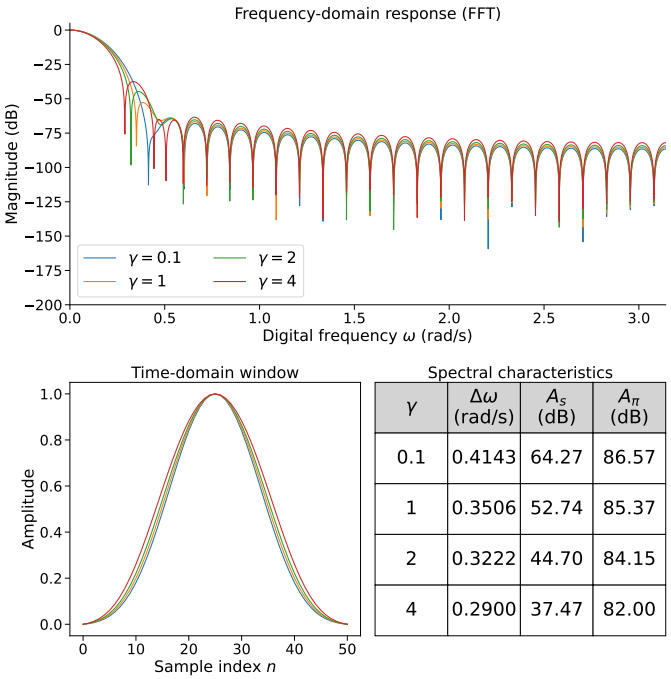

γ	$\Delta\omega$ (rad/s)	A_s (dB)	A_π (dB)
0.1	0.4143	64.27	86.57
1	0.3506	52.74	85.37
2	0.3222	44.70	84.15
4	0.2900	37.47	82.00

Fig. 3: Dependence of filter characteristics on γ when α = 0.8, β = 1 and σ = 0.913.

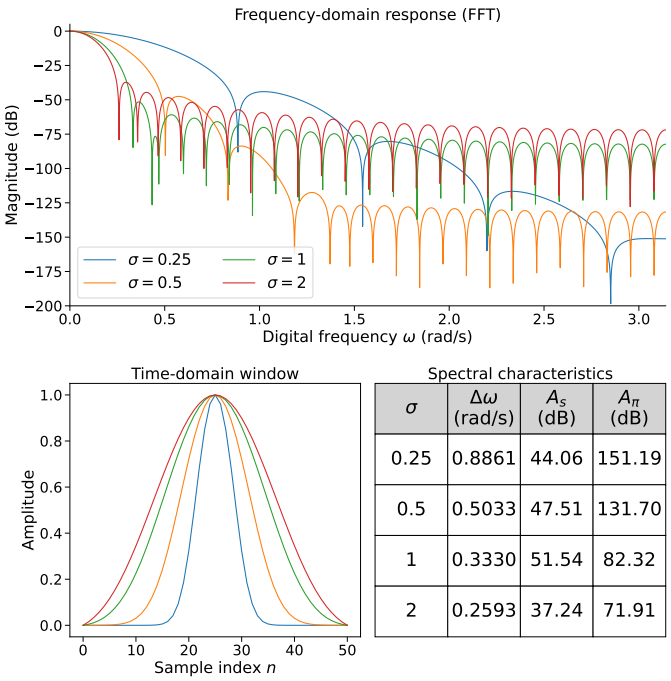

σ	$\Delta\omega$ (rad/s)	A_s (dB)	A_π (dB)
0.25	0.8861	44.06	151.19
0.5	0.5033	47.51	131.70
1	0.3330	51.54	82.32
2	0.2593	37.24	71.91

Fig. 4: Dependence of filter characteristics on σ when α = 0.8, β = 1 and γ = 1.

side-lobe decay, while a larger σ reduces roll-off and narrows the main-lobe width.

1) Comparative Analysis

A comparative analysis of the proposed window against the Hamming window [1], Taylor window [18], Dolph-Chebyshev window [12], Blackman-Harris window [9], the Kaiser window [13], and the Fractional-Kaiser window [17] for two window lengths ($M = 51$ and $M = 31$) is performed in this section. The metrics of comparison are chosen to be the half main-lobe width $\Delta\omega$, the first side-lobes attenuation A_s, and the attenuation at $\pi/2$ rad/sample, denoted by $A_{\pi/2}$. For higher spectral resolution, we use a 2000-point FFT.

From the figures 5, 6 and the data from the tables I and II, the window's targeted suppression strategy is evident, wherein the near side-lobes are attenuated to levels akin to that of the Kaiser, Dolph-Chebyshev and the Taylor windows while preserving a much narrower main-lobe width which is similar to or narrower than that of the Hamming window. Additionally,

TABLE I: Comparative Analysis of Different Windows ($M = 51$)

Window	Parameter Values	$\Delta\omega$ (rad/s)	A_s (dB)	$A_{\pi/2}$ (dB)
Hamming [1]	**nil**	0.2578	-47.64	-50.99
Taylor [18]	$\bar{n}$ = 3 sll = 67	0.2749	-60.73	-52.16
Proposed	α = 0.19 β = 0 γ = 0.82 σ = 0.850	0.2631	-61.43	-54.03
Chebyshev [12]	A = 61.27	0.3144	-61.27	-66.17
Kaiser [13]	α = 8.298	0.3543	-60.72	-81.42
Fractional Kaiser [17]	α = 5.7 γ = 0.74	0.3545	-63.11	-73.43
Proposed	α = 0.35 β = 0.21 γ = 0.8 σ = 0.79	0.3465	-80.28	-61.69
Blackman–Harris [9]	**nil**	0.5063	-101.74	-103.45

TABLE II: Comparative Analysis of Different Windows ($M = 31$)

Window	Parameter Values	$\Delta\omega$ (rad/s)	A_s (dB)	$A_{\pi/2}$ (dB)
Hamming [1]	**nil**	0.4403	-50.33	-47.36
Taylor [18]	$\bar{n}$ = 3 sll = 67	0.4533	-61.26	-48.01
Proposed	α = 0.01 β = 0 γ = 0.25 σ = 0.877	0.4107	-61.27	-47.41
Chebyshev [12]	A = 61.27	0.5220	-61.28	-62.64
Kaiser [13]	α = 8.40826	0.5972	-61.26	-80.223
Fractional Kaiser [17]	α = 5.65 γ = 0.74	0.5971	-63.42	-75.02
Proposed	α = 0.39 β = 0.22 γ = 0.82 σ = 0.786	0.5869	-86.75	-57.45
Blackman–Harris [9]	**nil**	0.8428	-104.36	-93.18

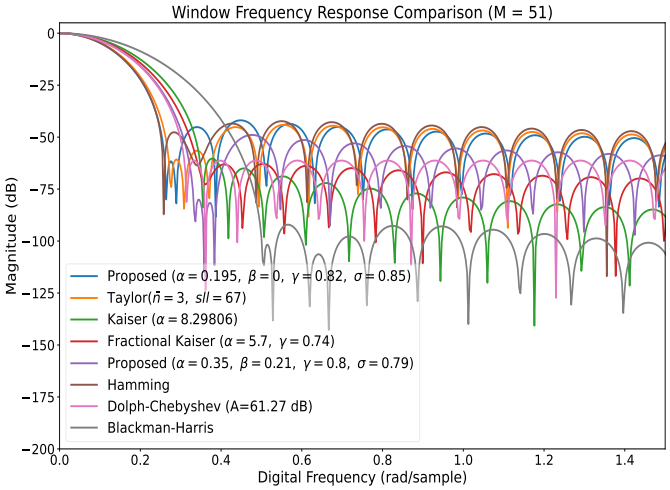

Fig. 5: Comparison of amplitude spectra of different windows for M = 51.

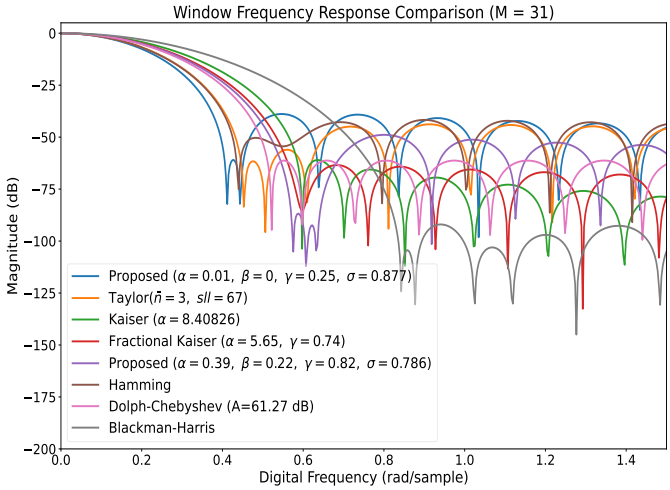

Fig. 6: Comparison of amplitude spectra of different windows for M = 31.

for roughly the same main-lobe width as the Kaiser and the fractional Kaiser window, the proposed window achieves more than 17 dB and 23 dB higher near-side-lobe attenuation than the fractional Kaiser window for $M = 51$ and $M = 31$ taps, respectively.

From the above results, it is evident that the proposed window can be tuned to enable it to strongly suppress the near-in-side-lobes, display an equi-ripple behavior or achieve an exponentially decaying side-lobe. This dynamic behavior makes it a suitable candidate for application in a variety of applications like image processing, biomedical signal processing, cognitive radio, radar applications, and communications, the demonstrations of which are within the future scope of this work. The parameter values have been selected using a hit-and-trial method to match the main-lobes and side-lobes of the existing windows. Development of a mathematical optimization technique for parameter selection is within the future scope of work as well.

IV. Conclusion

In this article, a novel four-parameter window formulated as a structured product of hyperbolic, exponential, and polynomial expressions is presented. The proposed window achieves attenuation levels comparable to those of the Taylor, Dolph–Chebyshev, and Kaiser windows while maintaining a narrower main-lobe width, and demonstrates superior near-in sidelobe suppression to the fractional Kaiser window at comparable main-lobe widths. Furthermore, it is shown that appropriate combinations of the four tuning parameters allow the window to exhibit targeted near-in sidelobe suppression, equiripple behavior, or exponential spectral decay. To our knowledge, this ability to realize distinct spectral behaviors within a unified four-parameter framework is uncharacteristic of existing window functions, making the proposed design suitable for a broad range of practical applications.

REFERENCES

[1] A. Antoniou, *Digital Signal Processing*. New York, NY, USA: McGraw-Hill, 2005.

[2] Gibbs, J. W., "Fourier's Series," *Nature*, vol. 59, p. 200, 1898.

[3] A. Chaudhary, *Image Fusion Methods and Applications: A Review*, Journal of Innovation and Technology, 2023.

[4] R. C. Gonzalez and R. E. Woods, *Digital Image Processing*, 4th ed. New York, NY, USA: Pearson Education, 2018.

[5] J. Zhang, T. Hu, X. Shao, M. Xiao, Y. Rong, and Z. Xiao, *Multi-Target Tracking Using Windowed Fourier Single-Pixel Imaging*, Sensors, vol. 21, p. 7934, 2021.

[6] N. S. Hashemi, R. B. Aghdam, A. S. Bayat Ghiasi, and P. Fatemi, *Template Matching Advances and Applications in Image Analysis*, arXiv:1610.07231, 2016.

[7] M. S. Bartlett, "Periodogram analysis and continuous spectra," *Biometrika*, vol. 37, no. 1/2, pp. 1–16, 1950.

[8] L. Sun and Y. Jitsumatsu, "Design of OTFS signals with pulse shaping and window function for OTFS-based radar systems," in *Proc. IEEE VTS Asia Pacific Wireless Communications Symposium (APWCS)*, Tokyo, Japan, 2025, pp. 1–5.

[9] F. J. Harris, "On the use of windows for harmonic analysis with the discrete Fourier transform," *Proc. IEEE*, vol. 66, no. 1, pp. 51–83, Jan. 1978.

[10] J. K. Gautam, A. Kumar, and R. Saxena, "On the modified Bartlett–Hanning window (family)," *IEEE Trans. Signal Process.*, vol. 44, no. 8, pp. 2098–2102, Aug. 1996.

[11] C. Lanczos, "Evaluation of noisy data," *J. Soc. Ind. Appl. Math. Ser. B Numer. Anal.*, vol. 1, no. 1, pp. 76–85, 1964.

[12] C. L. Dolph, "A current distribution for broadside arrays which optimizes the relationship between beam width and side-lobe level," *Proc. IRE*, vol. 34, no. 6, pp. 335–348, Jun. 1946.

[13] J. F. Kaiser, "Nonrecursive digital filter design using the I_0-sinh window function," in *Proc. IEEE Int. Symp. Circuits Syst. (ISCAS)*, 1974, pp. 20–23.

[14] K. Avcı, "Kaiser–Hamming window and its performance analysis for nonrecursive digital filter design," *J. Fac. Eng. Archit. Gazi Univ.*, vol. 29, no. 4, pp. 823–833, 2014.

[15] K. Avcı, "A new window function based on Kaiser and Von-Hann windows and its performance analysis for digital filter design," *Gazi Univ. J. Sci. Part C, Design Technol.*, vol. 5, no. 4, pp. 201–213, 2017.

[16] K. Avcı and A. Nacaroğlu, "High quality low order nonrecursive digital filters design using modified Kaiser window," in *Proc. 6th Int. Symp. Commun. Syst., Netw. Digit. Signal Process. (CSNDSP)*, Jul. 2008.

[17] K. Avcı, "Fractional Kaiser window with application to finite impulse response digital filter design," *IEEE Access*, vol. 12, pp. 155549–155563, 2024.

[18] T. T. Taylor, "Design of Line-Source Antennas for Narrow Beamwidth and Low Side Lobes", IRE Transactions on Antennas and Propagation, vol. 3, no. 1, pp. 16–28, 1955.

[19] R. Avanzato, F. Beritelli, G. Capizzi, and G. Lo Sciuto, "A new design methodology for window-based FIR filters," *Electronics Letters*, vol. 59, 2023.

[20] H. Xu and X. Suo, "A new type of window functions constructed with exponential function," arXiv preprint arXiv:2312.15267, 2023.

[21] A. Noureddine, M. Boussif, and C. Adnane, "A modified ultraspherical window and its application for speech enhancement," *Traitement du Signal*, vol. 39, no. 1, pp. 79–86, Feb. 2022.

[22] Y. C. Lim, Q. Liu, P. S. R. Diniz, and T. Saramäki, "Efficient design of scaled rectangular (Saramäki) window," *IEEE Signal Process. Lett.*, vol. 29, pp. 489–492, 2022.

[23] Sung JH, Jeong JS. Dual-/tri-apodization techniques for high frequency ultrasound imaging: a simulation study. Biomed Eng Online. 2014.

[24] M. Abdulsattar, "Energy detection technique for spectrum sensing in cognitive radio: A survey," Int. J. Comput. Netw. Commun., vol. 4, no. 5, pp. 223–242, Sep. 2012.

[25] Liu J, Wang W, Song H. Optimization of Weighting Window Functions for SAR Imaging via QCQP Approach. Sensors. 2020.

[26] S. V. Rao, A. Prasad, and C. S. Rani, "Antenna array weight synthesis for low side lobe levels using window functions," Int. J. Eng. Adv. Technol., vol. 9, pp. 3074–3081, Oct. 2019.